# Design of Two-Dimensional Crystals as Models for Probing the Structure of the Solid-Liquid Interface

**D. Gidalevitz,† I. Weissbuch,† K. Kjaer,‡ J. Als-Nielsen,*,‡ and L. Leiserowitz*,†**

*Contribution from the Department of Materials and Interfaces, The Weizmann Institute of Science, 76100 Rehovot, Israel, and Physics Department, Risø National Laboratory, DK4000 Roskilde, Denmark*

*Received July 12, 1993. Revised Manuscript Received February 14, 1994®*

**Abstract**: Crystals of β-alanine and the α-form of glycine, when grown in the presence of 3% molar $CdCl_2$, display morphologies which are different from those obtained from pure water solution. This effect was interpreted in terms of binding of $Cd^{2+}$ and $Cl^-$ ions to the exposed $CO_2^-$ and $NH_3^+$ moieties at the various faces, so changing their relative rates of growth and leading to the development of new faces. The structure of the crystal face of β-alanine most affected by the presence of $CdCl_2$ was mimicked by a monolayer containing an equimolar mixture of two different amphiphiles octadecylamine ($C_{18}H_{37}NH_2$) and stearic acid ($C_{17}H_{35}COOH$) spread on aqueous solution. Binding of the $Cd^{2+}$ and $Cl^-$ ions to such a monolayer has been investigated. X-ray specular reflectivity measurements reveal that the mixed monolayer is fully bound by $Cd^{2+}$ and $Cl^-$ ions when their concentration reaches 0.1 M. Grazing incidence X-ray diffraction measurements, using synchrotron radiation, of the mixed monolayer on pure water and on a 0.1 M $CdCl_2$ solution provide strong evidence that the monolayer $CO_2^-$ and $NH_3^+$ head groups are arranged in ordered array and the $Cd^{2+}$ and $Cl^-$ ions are bound to the monolayer head groups at ordered sites.

## 1. Introduction

Solvent and impurities have a pronounced effect on the growth and morphology of molecular crystals obtained from solution. There have been two schools of thought as to how solvent affects growth. One is that favorable interactions between solute and solvent on specific faces will lead to reduced interfacial tension, causing a transition from a smooth to a rough interface, and a concomitant faster surface growth.[1-4] Alternatively, it has been proposed that preferential adsorption of solvent molecules at specific faces will inhibit growth of those faces as removal of bound solvent molecule imposes an additional energy barrier for continued growth.[5-11] This proposed mechanism is also in keeping with the effect of stereospecific adsorption of "tailor made" molecular additives on growing crystal surfaces[12-15] or the effect of "tailored" cosolvent additives on the faces of crystalline solvates.[16] In both cases additives cause inhibition of growth perpendicular to the crystal surface, resulting in an increase of its surface area.

Although many experiments have been performed in which the crystal morphology can be understood in terms of strong binding of either solvent[5-11,16] or additive molecules[12-15] to specific faces, little work has been reported on the direct determination of the local structure at such a liquid–crystal interface.[17] Such information can, in principle, be obtained from surface X-ray diffraction. For such an experiment to have a reasonable chance of success, several requirements should be met. For example, the additive molecules should be strongly and specifically bound to a subset of different crystallographic sites on the crystal surface. The solute molecules should be small in size so that the concentration of surface sites be as high as possible and should be light X-ray scatterers in comparison to the additive.

We thus chose as model crystals the α-form of glycine ($^+H_3NCH_2CO_2^-$) and β-alanine ($^+H_3NCH_2CH_2CO_2^-$) and as additive $Cd^{2+}$ and $Cl^-$ ions. The crystals of both α-glycine and β-alanine, when grown from aqueous solution, develop faces which expose zwitterionic carboxylate ($CO_2^-$) and amino ($NH_3^+$) groups. It is a simple matter, as we shall show, to demonstrate the effect of the $Cd^{2+}$ and $Cl^-$ ions on the morphology of these crystals and to qualitatively correlate the change in morphology with the surface structure of the crystals. But to provide direct structural information on the lateral arrangement of the ions bound to the crystal surface by grazing incidence X-ray diffraction (GID) or specular X-ray reflectivity (XR) is still a formidable task, because a large and smooth crystal face and a very thin liquid layer in equilibrium with the crystal would be required to obtain an appreciable signal-to-noise ratio. In order to circumvent such difficulties, we made use of an equimolar mixture of the long-chain fatty acid $C_{17}H_{35}CO_2H$ and the amine $C_{18}H_{37}NH_2$ spread as monolayer on various liquid subphases, so as to mimic the most affected face of the crystals. The ion binding to the monolayer was probed by XR and GID techniques.

* Author to whom correspondence should be addressed.
† The Weizmann Institute of Science.
‡ Risø National Laboratory.
• Abstract published in *Advance ACS Abstracts*, January 1, 1994.
(1) Bennema, P.; Gilmer, G. In *Crystal Growth; An Introduction*; Hartman, P., Ed.; North-Holland: Amsterdam, 1973; p 272.
(2) Bourne, J. R.; Davey, R. J. *J. Cryst. Growth* **1976**, *36*, 287.
(3) Elwenspoek, M.; Bennema, P.; Eerden, J. P. v. d. *J. Cryst. Growth* **1987**, *83*, 297.
(4) Bennema, P.; Eerden, J. P. v. d. In *Morphology of Crystals*; Terra Scientific Publishing Co.: Tokyo, 1987; pp 1–75.
(5) Wells, A. F. *Philos. Mag.* **1946**, *37*, 184.
(6) Wells, A. F. *Discuss Faraday Soc.* **1949**, *5*, 197.
(7) Wireko, F. C.; Shimon, L. J. W.; Frolow, F.; Berkovitch-Yellin, Z.; Lahav, M.; Leiserowitz, L. *J. Phys. Chem.* **1987**, *91*, 472.
(8) Berkovitch-Yellin, Z. *J. Am. Chem. Soc.* **1985**, *107*, 8239.
(9) Davey, R. J. *J. Cryst. Growth* **1986**, *76*, 637.
(10) Davey, R. J.; Milisavljevic, B.; Bourne, J. R. *J. Phys. Chem.* **1988**, *92*, 2032.
(11) Wang, J.-L.; Leiserowitz, L.; Lahav, M. *J. Phys. Chem.* **1992**, *96*, 15–16.
(12) Addadi, L.; Weiner, S. *Proc. Natl. Acad. Sci. U.S.A.* **1985**, *82*, 4110.
(13) Addadi, L.; Berkovitch-Yellin, Z.; Weissbuch, I.; Lahav, M.; Leiserowitz, L. In *Topics in Stereochemistry*; Wiley: New York, 1986; Vol. 16, pp 1–85.
(14) Shimon, L. J.; Lahav, M.; Leiserowitz, L. *Nouv. J. Chim.* **1986**, *10*, 723–737.
(15) Weissbuch, I.; Addadi, L.; Lahav, M.; Leiserowitz, L. *Science* **1991**, *253*, 637–645.
(16) Shimon, L. J. W.; Vaida, M.; Addadi, L.; Lahav, M.; Leiserowitz, L. *J. Am. Chem. Soc.* **1990**, *112*, 6215–6220.
(17) Cunningham, D. A. H.; Davey, R. J.; Roberts, K. J.; Sherwood, J. N.; Shripathi, T. *J. Cryst. Growth* **1990**, *99*, 1065–1069. Cunningham, D. A. H.; Armstrong, D. R.; Clydesdale, G.; Roberts, K. J. *Faraday Discuss.*, in press.

0002-7863/94/1516-3271$04.50/0 

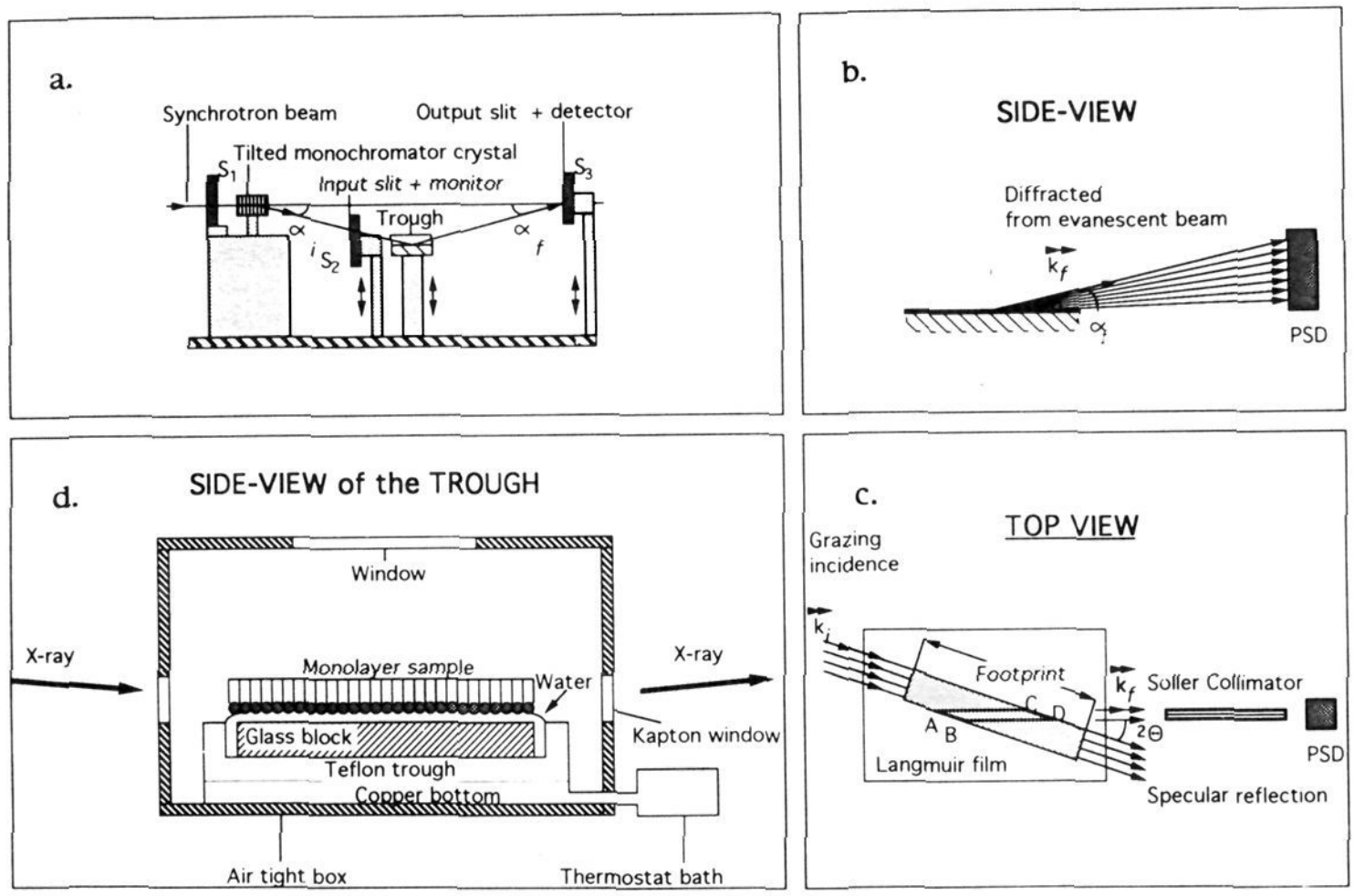


**Figure 1.** Experimental setup of a liquid surface diffractometer (beamline D4, X-ray synchrotron source at Hasylab, Hamburg). (a and b) Side view of the vertical scattering phase. Beam directions are defined by slits. The monochromatic beam is bent down toward the sample by tilting the monochromator crystal. The incident beam intensity is monitored after slit $S_2$. (c) Top view of GID geometry. The footprint of the grazing incidence beam is delineated. The position-sensitive detector (PSD) has its axis along the vertical direction. Only the area ABCD contributes to the scattering. $\mathbf{k}_i$ and $\mathbf{k}_f$ are the incident and outgoing wave vectors. The scattering vector $\mathbf{q}$ ($= \mathbf{q}_{xy} + \mathbf{q}_z$) is given by $\mathbf{k}_f - \mathbf{k}_i$. The vertical scattering vector $\mathbf{q}_z = 2\pi \sin \alpha_f/\lambda$, where $\alpha_f$ is depicted in (b); the horizontal scattering vector $\mathbf{q}_{xy} = 4\pi \sin \theta/\lambda$, where $\theta$ is the Bragg angle. (d) Blown-up view of the trough showing the monolayer sample spread on a thin film of water. The glass block provides for a thin liquid film (about 0.3 mm thick) and thus effectively reduces surface capillary waves.

## 2. Experimental Section

**Materials.** For the crystallization experiments we made use of glycine ($NH_2CH_2CO_2H$) and β-alanine ($NH_2(CH_2)_2CO_2H$) both from Fluka (purity > 99%). Cadmium chloride monohydrate ($CdCl_2 \cdot H_2O$, purity > 98%), calcium chloride dihydrate ($CaCl_2 \cdot 2H_2O$, purity > 99%), zinc chloride ($ZnCl_2$, purity > 98%), cesium bromide (CsBr, purity > 99.5%), rubidium chloride (RbCl, purity > 99.5%), and barium chloride dihydrate ($BaCl_2 \cdot 2H_2O$, purity > 99%) were from Merck and have been used as additives.

As monolayer amphiphiles we used octadecylamine ($CH_3(CH_2)_{17}NH_2$, Fluka, purity 99%) and stearic acid ($CH_3(CH_2)_{16}CO_2H$, Merck, purity 99%). For subphase solutions we used the same β-alanine and cadmium chloride monohydrate as for crystallization experiments and cadmium bromide tetrahydrate ($CdBr_2 \cdot 4H_2O$, Fluka, purity > 97%). Spreading solutions of amphiphiles were prepared as an equimolar mixture in chloroform (Merck, analytical grade) with total concentration of $10^{-3}$ M. The water used in both crystallization and monolayer experiments was Millipore grade.

**Crystal Growth and Morphology.** The crystals of the α-form of glycine and of β-alanine were grown as follows. Seeds, obtained from hot, supersaturated solution by slow evaporation, were placed in a fresh supersaturated aqueous solution of the compound at a temperature of 40–42 °C. The solution was cooled at a rate of 1 deg/day down to a temperature of 10 °C, yielding large crystals with dimensions up to 30 mm. Crystals were also grown by the same procedure in the presence of various salts ($CdCl_2$, $ZnCl_2$, $CaCl_2$, CsBr, RbCl, $BaCl_2$) as cosolutes. In general, the salt concentration was in a range 2–3 mol %.

**Experimental Setup for X-ray Reflectivity and Grazing Incidence Diffraction Measurements.** The X-ray scattering experiments on the monolayers on the liquid surface were carried out on two instruments. The XR measurements were made on a liquid surface X-ray reflectometer.[18] The grazing incidence diffraction (GID) data were collected on the liquid surface diffractometer (Figure 1) at the synchrotron X-ray beamline D4 at Hasylab, DESY, Hamburg, Germany. The experimental setup of this diffractometer has been described elsewhere in detail.[19-23] A sealed and thermostated Langmuir trough equipped with a Willhelmy balance, allowing for surface pressure control of the film, was mounted on the diffractometer. The synchrotron radiation beam was monochromated to a wavelength $\lambda = 1.38$ Å, and to maximize surface sensitivity, the incident beam was adjusted to strike the monolayer surface at an angle $\alpha_i = 0.85\alpha_c$, where $\alpha_c = 0.138°$ is the critical angle for total external reflection. The dimensions of the footprint of the incoming X-ray beam on the liquid surface were $50 \times 5$ mm$^2$. Detection of the outgoing X-ray beam for GID measurements was made by a linear position-sensitive detector (PSD), whereas for XR measurements it was made with a scintillation detector. The setup of the X-ray reflectometer mounted on a rotating copper anode is similar in principle to the one at beamline D4. The angle of the incident beam was varied from $0.5\alpha_c$ to $20\alpha_c$.

**X-ray Scattering Experiments.** Two sets of X-ray reflectivity experiments on the equimolar mixture of $C_{18}H_{37}NH_2$ and $C_{17}H_{35}CO_2H$ were performed. For one set the monolayer mixture was spread on aqueous solution subphases containing different concentrations of $CdCl_2$ and $CdBr_2$ in the range $10^{-3}$–0.1 M at 5 °C to investigate their ability to bind to the monolayer. In order to obtain information on the effect of β-alanine dissolved in the subphase, a second set of XR experiments were made. These involved the use of 2.1 and 4.1 M β-alanine solutions, with and without 0.1 M $CdCl_2$ additive. The β-alanine concentrations are comparable to those used in its crystallization experiments.

Grazing incidence diffraction experiments were aimed at determining the monolayer structure at the air–liquid interface. The GID measurements were performed on monolayer mixtures spread at 5 °C on pure

(18) Als-Nielsen, J. *X-ray Reflectivity Studies of Liquid Surfaces*; Handbook of Synchrotron Radiation 3; North Holland: Amsterdam; 1991.

(19) Helm, C. A.; Möhwald, H.; Kjaer, K.; Als-Nielsen, J. *Biophys. J.* **1987**, *52*, 381.
(20) Grayer Wolf, S.; Leiserowitz, L.; Lahav, M.; Deutsch, M.; Kjaer, K.; Als-Nielsen, J. *Nature* **1987**, *328*, 63.
(21) Grayer Wolf, S.; Landau, E. M.; Lahav, M.; Leiserowitz, L.; Deutsch, M.; Kjaer, K.; Als-Nielsen, J. *Thin Solid Films* **1988**, *159*, 29.
(22) Jacquemain, D.; Grayer Wolf, S.; Leveiller, F.; Lahav, M.; Leiserowitz, L.; Deutsch, M.; Kjaer, K.; Als-Nielsen, J. *J. Am. Chem. Soc.* **1990**, *112*, 7724.
(23) Jacquemain, D.; Grayer Wolf, S.; Leveiller, F.; Deutsch, M.; Kjaer, K.; Als-Nielsen, J.; Lahav, M.; Leiserowitz, L. *Angew. Chem.* **1992**, *31*, 130–152.

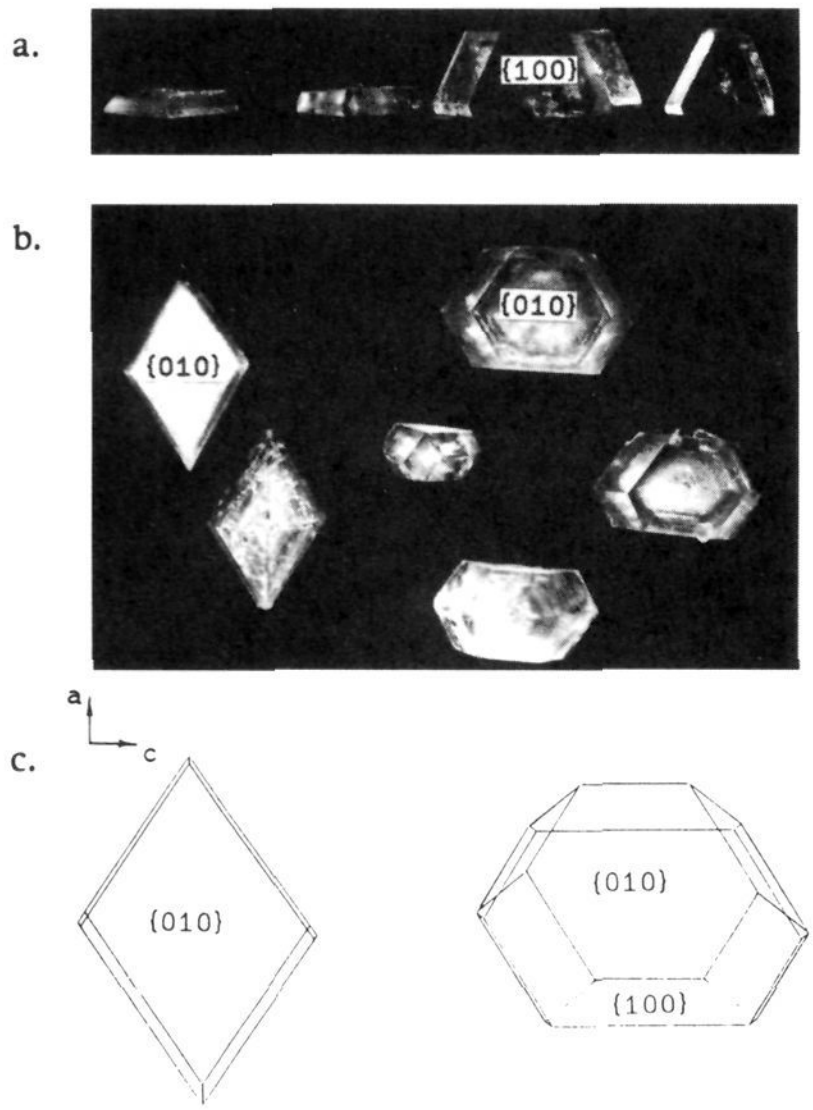


**Figure 2.** Morphologies of $\beta$-alanine crystals grown (left) from pure solution and (right) in the presence of 3 mol % $CdCl_2$. The {*hkl*} indices of the faces are shown. (a and b) Photographs of top and side views of the pure and affected $\beta$-alanine crystals. (c) Computer-drawn morphology of the $\beta$-alanine crystals.

water, 0.1 M $CdCl_2$ solution, and subphase containing 4.2 M $\beta$-alanine and 0.1 M $CdCl_2$.

## 3. Results and Discussion

**3.1 Crystal Growth Experiments. $\beta$-Alanine.** This compound, which crystallizes in the orthorhombic space group *Pbca* with cell dimensions[24,25] $a = 9.87$ Å, $b = 13.81$ Å, $c = 6.07$ Å, grows as thin {010} plates from aqueous solutions. The largest crystals grown from pure solution reached dimensions $30 \times 3 \times 20$ mm$^3$, exhibiting {010} and {111} faces. There was a gradual change in morphology when crystals were grown from solutions containing increased concentration of salt additives $CdCl_2$, $ZnCl_2$, and $CaCl_2$. The crystals grew much thicker along the *b* direction and displayed {010}, {100}, and {111} faces. Morphologies of the specimen crystals are presented in Figure 2. The most dramatic effect was obtained with $CdCl_2$ additive, yielding well-developed {100} faces. Their appearance can be explained on a molecular level. The {100} face (Figure 3) has the highest concentration of exposed $CO_2^-$ and $NH_3^+$ groups and thus should bind the largest amount of $Cd^{+2}$ and $Cl^-$ ions. This adsorbed $Cd^{2+}$ and $Cl^-$ layer should inhibit growth perpendicular to the underlying {100} face, resulting in its increased morphological importance relative to other faces.

**Glycine.** Crystals of the $\alpha$-form of glycine are monoclinic, space group $P2_1/n$, with the following cell dimensions:[26] $a = 5.08$ Å, $b = 11.82$ Å, $c = 5.46$ Å, and $\beta = 112.0°$. The crystals grow from pure aqueous solution as bipyramids expressing {110}, {011}, and {010} faces (Figure 4). Generally, the {110} face is morphologically more important than {011}, and the {010} face is poorly expressed. The presence of 2 mol% $CdCl_2$ in solution caused a significant change in crystal shape, displaying {120} and {210} faces instead of {110} and an increased morphological importance of the {011} faces (Figure 4). This result can be explained on a molecular level. The {110} face is not as molecularly smooth as the {120} face. The appearance of the former when grown from the pure solution can be understood in terms of surface docking of centrosymmetrical hydrogen-bonded glycine dimers (see Figure 5); the development of the smoother {120} face (Figure 5) in the presence of $CdCl_2$ suggests that solute glycine docks as single molecules. The increased morphological importance of {011} may be correlated with the fact that this face exposes the highest concentration of $CO_2^-$ and $NH_3^+$ groups, as was also found for affected $\beta$-alanine.

**3.2 Binding of $CdCl_2$ and $^+H_3NC_2H_4CO_2^-$ to the Mixed Monolayer.** The equimolar mixture of $C_{18}H_{37}NH_2$ and $C_{17}H_{35}CO_2H$ spread as a monolayer on an aqueous solution was designed to form a surface which would mimic the {100} crystal surface of $\beta$-alanine. As already alluded to, the monolayer–liquid interface would be more amenable to study by surface X-ray scattering methods than the {100} face of $\beta$-alanine for the following reasons: the monolayer surface can be easily prepared, is perfectly smooth over a wide area, and would not be adversely affected by ions or $\beta$-alanine molecules in solution. Most importantly, the measured X-ray beam scattered from the monolayer would not pass through bulk solution and so would not suffer from a high background noise as might be expected with a crystal of $\beta$-alanine covered by solution.

The {100} face of $\beta$-alanine (Figure 3) consists of alternating double rows of $CO_2^-$ and of $NH_3^+$ moieties parallel to the *c* axis. Clearly, the equimolar mixture of octadecylamine and stearic acid cannot mimic the double-row structure of the {100} face, but we may expect, at least, alternating rows of ordered $CO_2^-$ and $NH_3^+$ head groups of the mixed monolayer, sufficient for studying the binding of ions and competitive binding of $\beta$-alanine solute molecules.

**Analysis of the X-ray Reflectivity Data.** The measured X-ray reflectivity curves from the uncompressed monolayer mixture over pure water and over solutions containing different concentrations of $CdCl_2$ and $CdBr_2$ salts are given in Figure 6a.

The calculated reflectivity curves[27] were obtained according to a two-box molecular model[28] with parameters presented in Table 1. We have assumed that the interface may be adequately described in terms of two boxes (Figure 7): the box of electron density $\rho_H$ and length $L_H$ models the head groups of the monolayer mixture (each component with 50% occupancy) and the bound ions; the second box, of electron density $\rho_T$ and length $L_T$, models the hydrocarbon tails. For the pure water subphase, an excellent fit was obtained with the molecules vertically aligned, an area per molecule of $A = 19.5$ Å$^2$, and one water molecule per amphiphile molecule.

The X-ray reflectivity curves of the mixed monolayer spread over $CdCl_2$ solution were measured in the concentration range from $10^{-3}$ to $10^{-1}$ M (Figure 6a). Complete coverage of $Cd^{2+}$ and $Cl^-$ ions bound to the monolayer head groups is achieved only for the maximum 0.1 M $CdCl_2$ concentration, according to the fitting analysis (Table 1). The structural model consists of one bound $Cd^{2+}$ ion per two carboxylate $CO_2$ head groups and one bound $Cl^-$ ion per amine $NH_3$ head group. We deduce from analysis of the X-ray reflectivity results that the surface electrostatic potential from an ordered array of $CO_2^-$ and $NH_3^+$ head groups is not sufficiently strong at $CdCl_2$ concentrations well below 0.1

(24) Jose, P.; Pant, L. M. *Acta Crystallogr.* **1964**, *18*, 806–810.
(25) Papavinasam, E.; Natarajan, S.; Shivaprakash, N. S. *Int. J. Pept. Protein Res.* **1986**, *28*, 525–528.
(26) Legros, J.-P.; Kvick, ·. *Acta Crystallogr.* **1980**, *B36*, 3052–3059.

(27) The X-ray specular reflectivity is governed by the followiing formula:

$$\frac{R(\mathbf{q}_z)}{R_F(\mathbf{q}_z)} = \left|\int \rho'(z) \exp(i\mathbf{q}_z)\, dz\right|^2$$

$R/R_F$ is the measured reflectivity divided by the Fresnel reflectivity calculated for a perfect, sharp interface: $\rho'(z)$ denotes the gradient of the electron density, $\rho(z)$, perpendicular to the surface; $\mathbf{q}_z/\mathbf{q}_c$ is the normalized vertical scattering vector, where $\mathbf{q}_z = 4\pi \sin\theta/\lambda$ and $\mathbf{q}_c$ is the scattering vector at the critical angle of incidence.

(28) Kjaer, K.; Als-Nielsen, J.; Helm, C. A.; Tippman-Krayer, P.; Möhwald, H. *J. Phys. Chem.* **1989**, *93*, 3200.

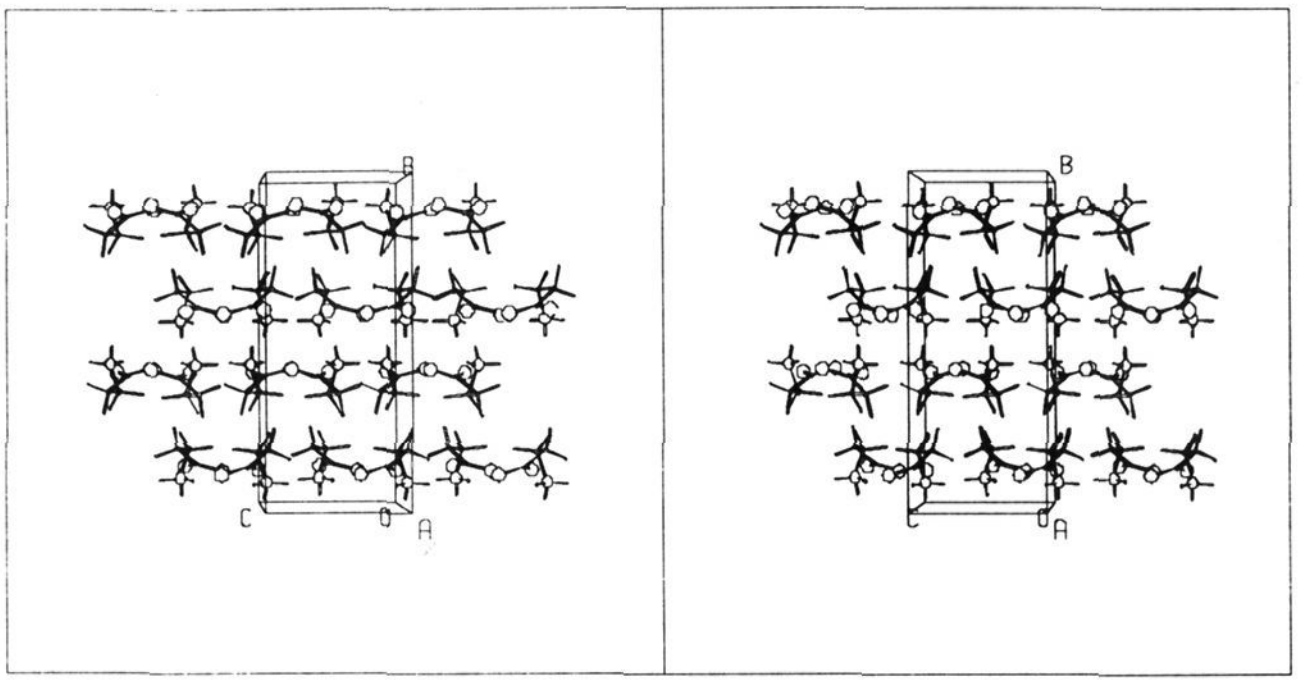


**Figure 3.** Stereoscopic view of the crystalline packing arrangement of the $\beta$-alanine crystal seen along the $a$ axis. Note that the $CO_2^-$ and $NH_3^+$ moieties of the (100) crystal face are exposed.

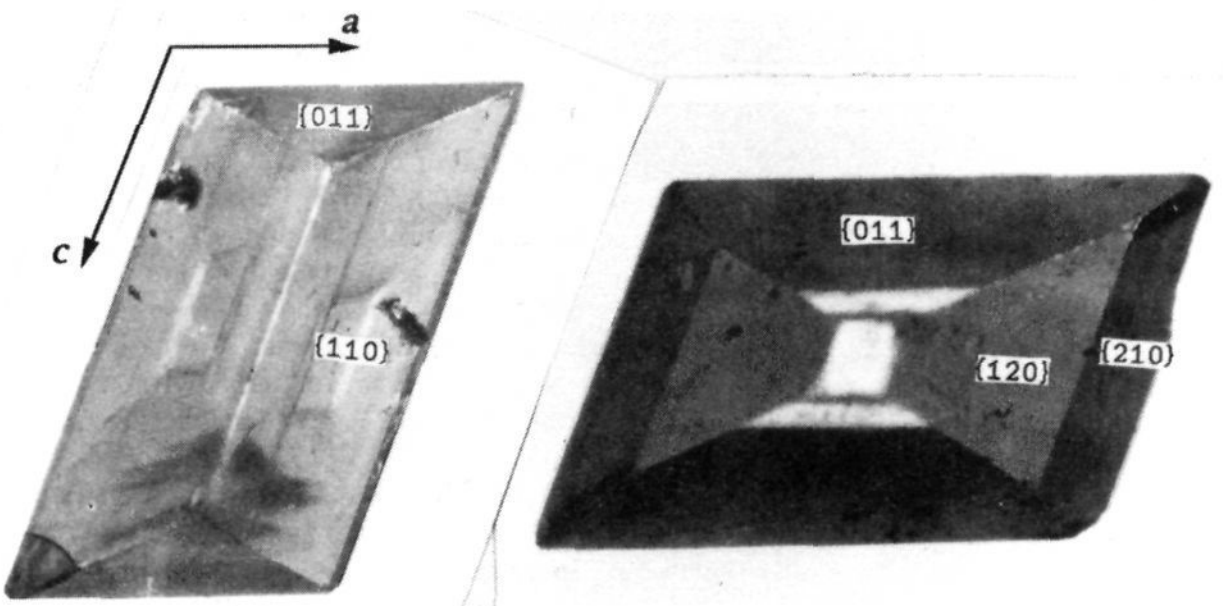


**Figure 4.** Photographs of the $\alpha$-form of glycine grown (left) from pure glycine solution and (right) in the presence of 3 mol % $CdCl_2$. The $\{hkl\}$ indices of the crystal faces are indicated.

M to induce complete binding of the counterions. This observation is, as expected, different from the X-ray reflectivity measurements on arachidic acid monolayers spread on $CdCl_2$ subphases,[28] where complete $Cd^{2+}$ ion binding occurred at $10^{-3}$ M concentration at pH = 6.5. In the latter case, the electrostatic potential induced by the $CO_2^-$ head groups at the interface is much higher. In modeling the X-ray reflectivity curve for the subphase containing $CdBr_2$ (Figure 6a), the best fit was obtained for complete ion binding as for $CdCl_2$.

The second set of X-ray reflectivity measurements illustrates the effect of competitive binding of $\beta$-alanine dissolved in the subphase. The X-ray reflectivity curves for the mixed monolayer spread over subphases containing 0.1 M $CdCl_2$ (required for complete $Cd^{2+}$ and $Cl^-$ binding) and various amounts of $\beta$-alanine are depicted in Figure 6b. We chose $\beta$-alanine concentrations of 2.1 and 4.2 M because these are comparable to those used in the 3-D crystallization experiments. A three-box model has been used for fitting the data. The box with electron density $\rho_{\beta A}$ and length $L_{\beta A}$ models the bound $\beta$-alanine and water molecules; the second and third boxes model the head groups and hydrocarbon chains, respectively (Table 1). There is a distinct difference in the observed reflectivity curves from the monolayer over pure water and 4.2 M $\beta$-alanine solution (Figure 6c). These curves were well fit assuming complete binding of $\beta$-alanine. However, the small difference of $\sim$4% between the electron density of the bulk subphase and that of the bound $\beta$-alanine layer does suggest a large margin of error. The measured reflectivity curves (Figure

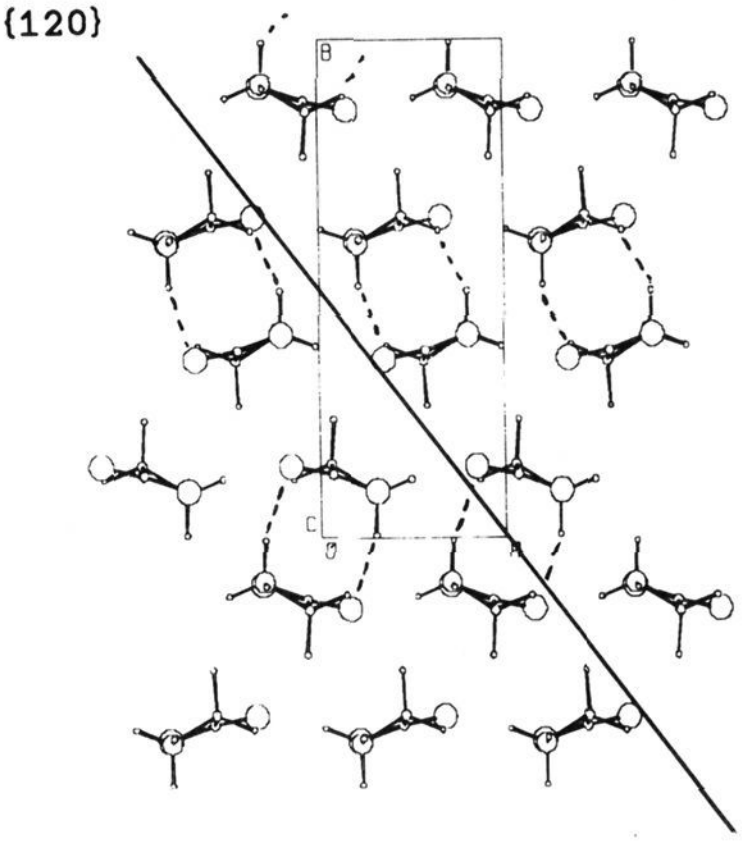


**Figure 5.** Packing arrangement of the $\alpha$-form of glycine viewed along the $c$ axis. The cyclic dimers formed by hydrogen bonds (···) are shown. The (120) plane is indicated.

6b) indicate that addition of $\beta$-alanine molecules to the subphase solutions containing 0.1 M $CdCl_2$ causes a competitive binding

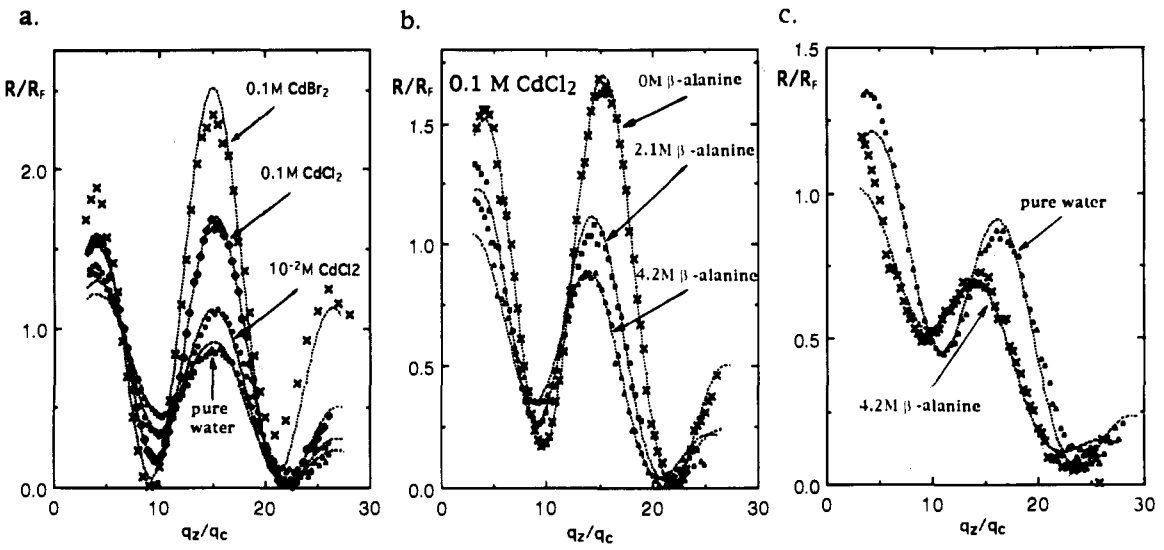


**Figure 6.** Measured (points) and calculated (dotted line) X-ray specular reflectivities[27,36] from an uncompressed monolayer of equimolar mixtures of octadecylamine ($C_{18}H_{37}NH_2$) and stearic acid ($C_{17}H_{35}CO_2H$) over aqueous subphases at 5 °C containing the following solutes: (a) $CdCl_2$ or Cd $Br_2$ in the concentration range 0–0.1 M, (b) a fixed 0.1 M $CdCl_2$ concentration and β-alanine in the range 0–4.2 M, and (c) pure water and 4.2 M β-alanine.

**Table 1.** Fitted Parameters for the Box Model of Electron Density Corresponding to the X-ray Reflectivity Curves Shown in Figure 6[a]

| subphase | no. of boxes | $\rho_s$ (e/Å$^3$) | $A$ (Å$^2$) | $\rho_{\beta A}/\rho_s$ | $L_{\beta A}$ (Å) | $\rho_H/\rho_s$ | $L_H$ (Å) | $\rho_T/\rho_s$ | $L_T$ (Å) | $\sigma$ (Å) |
|---|---|---|---|---|---|---|---|---|---|---|
| water | 2 | 0.334 | 19.5 | | | 1.377 | 2.9 | 0.999 | 21.5 | 2.6 |
| $10^{-3}$ M $CdCl_2$ | 2 | 0.334 | 19.5 | | | 1.480 | 2.9 | 0.999 | 21.5 | 2.6 |
| $10^{-2}$ M $CdCl_2$ | 2 | 0.335 | 19.5 | | | 1.531 | 2.9 | 0.997 | 21.5 | 2.5 |
| $10^{-1}$ M $CdCl_2$ | 2 | 0.337 | 19.5 | | | 1.887 | 3.0 | 0.991 | 21.5 | 2.6 |
| $10^{-1}$ M $CdBr_2$ | 2 | 0.340 | 19.5 | | | 2.102 | 3.3 | 0.985 | 21.6 | 2.4 |
| 4.2 M β-alanine | 3 | 0.363 | 19.5 | 1.037 | 6.4 | 1.266 | 2.9 | 0.948 | 21.0 | 2.8 |
| 4.2 M β-alanine + $5 \times 10^{-2}$ M $CdCl_2$ | 3 | 0.366 | 19.5 | 1.029 | 6.4 | 1.449 | 2.9 | 0.982 | 21.0 | 2.8 |
| 4.2 M β-alanine + $10^{-1}$ M $CdCl_2$ | 3 | 0.368 | 19.5 | 1.023 | 6.4 | 1.490 | 2.9 | 0.941 | 21.0 | 2.8 |
| 2.1 M β-alanine | 3 | 0.350 | 19.5 | 1.053 | 6.4 | 1.314 | 2.9 | 0.967 | 21.1 | 2.9 |
| 2.1 M β-alanine + $10^{-1}$ M $CdCl_2$ | 3 | 0.354 | 19.5 | 1.051 | 6.2 | 1.548 | 2.9 | 0.976 | 21.1 | 2.8 |

[a] $\rho_s$ is the electron density of the subphase; $A$ is the molecular area; $\rho_{\beta A}$, $\rho_H$, $\rho_T$ are the model electron densities of the first, second, and third boxes, respectively; $L_{\beta A}$, $L_H$, and $L_T$ are the lengths of the boxes, respectively; $\sigma$ represents the surface roughness parameter.

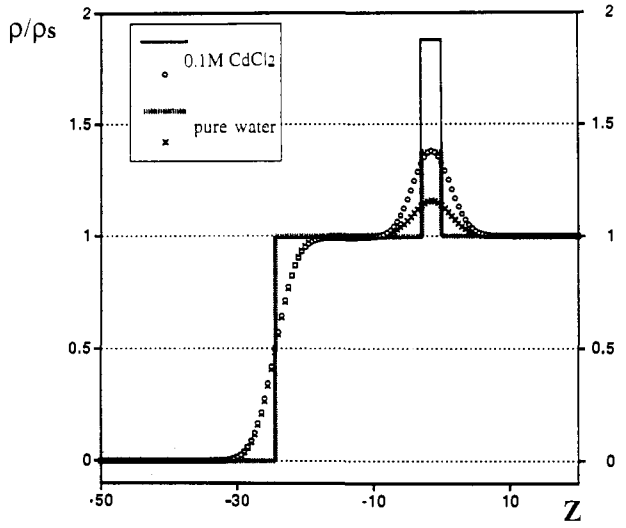


**Figure 7.** Refined relative electron density $\rho/\rho_s$ ($\rho_s$ is the electron density of the subphase) profiles of mixed monolayer over pure water and 0.1 M $CdCl_2$ aqueous solution assuming the two-box model. The model density is smeared by a Gaussian parameter $\sigma$ (see Table 1).

in keeping with a decrease in the calculated electron density of the bound β-alanine–$Cd^{2+}$,$Cl^-$ layer. (Table 1).

**Analysis of the Grazing Incidence X-ray Diffraction Data.** The GID pattern from the equimolar mixture of stearic acid and octadecylamine spread over water at 5 °C and maintained at a constant surface pressure of 30 mN/m shows two peaks (Figure 8a) of approximately equal intensity at $q_{xy}$ = 1.490 and 1.627 Å$^{-1}$. These two peaks were indexed as the {1,1} + {1,$\bar{1}$} and {0,2} reflections from a rectangular unit cell, yielding axial dimensions $a$ = 5.03 Å, $b$ = 7.73 Å, $\gamma$ = 90°, and so an area per molecule of $A$ = 19.4 Å$^2$. Similar cell dimensions have been reported for many other amphiphiles $C_nH_{2n+1}X$ (X = polar group) in which the chains tend to be vertically aligned[29] and is indicative of a "herringbone" arrangement of the hydrocarbon chains, generated by glide symmetry and commonly described as the orthogonal O⊥ motif.[30,31] The observed Bragg rod intensity profiles of the monolayer spread over water (Figures 9a) indicate that the molecules are aligned approximately vertically. We propose two model structures I and II containing ordered arrangements of molecules of $C_{18}H_{37}NH_3^+$ and $C_{17}H_{35}CO_2^-$ as shown on Figure 10a,b. In model I molecules of the same kind are related by

(29) Jacquemain, D.; Leveiller, F.; Weinbach, S.; Lahav, M.; Leiserowitz, L.; Kjaer, K.; Als-Nielsen, J. *J. Am. Chem. Soc.* **1991**, *113*, 7684–7691.
(30) Small, D. M. In *Handbook of Lipid Research*; Plenum Press: New York, 1986; Vol. 4, Chapter 4, pp 2, 5, 8.
(31) Kitaigorodski, A. I. *Organic Chemical Crystallography*; Consultants Bureau Press: New York, 1961; Ch. 4; pp 117.
(32) The structure factor $F_{hk}(q_z)$ is given by:

$$F_{hk}(q_z) = \sum_j f_j \exp\{i(q_{hk}\cdot r_j + q_z z_j)\}$$

where $f_j$ is the scattering factor of the atom $j$; $r_j = x_j a + y_j b$ is the vector specifying the $(x,y)$ position of the atom $j$ in the unit cell of dimensions $a,b$; and $z_j$ is the atomic coordinate in angstroms along the vertical direction and $q_{hk} = (4\pi/\lambda)\sin\theta_{hk}$.

(33) Als-Nielsen, J.; Kjaer, K. *Proceedings of the NATO Advanced Study Institute, Phase Transitions in Soft Matter*; Geilo, Norway, April 4–14, 1989; Riste, T. Sherrington, D., Eds.; Plenum Press: New York, London, 1989; pp 113–137.
(34) Jacquemain, D.; Grayer Wolf, S.; Leveiller, F.; Lahav, M.; Leiserowitz, L.; Deutsch, M.; Kjaer, K.; Als-Nielsen, J. *Colloq. Phys.* **1989**, *C7*, 29.
(35) Feidenhans'l, R. *Surf. Sci. Rep.* **1989**, *10*(3), 105.
(36) Leveiller, F.; Jacquemain, D.; Lahav, M.; Leiserowitz, L.; Deutsch, M.; Kjaer, K.; Als-Nielsen, J. *Science* **1991**, *252*, 1532.

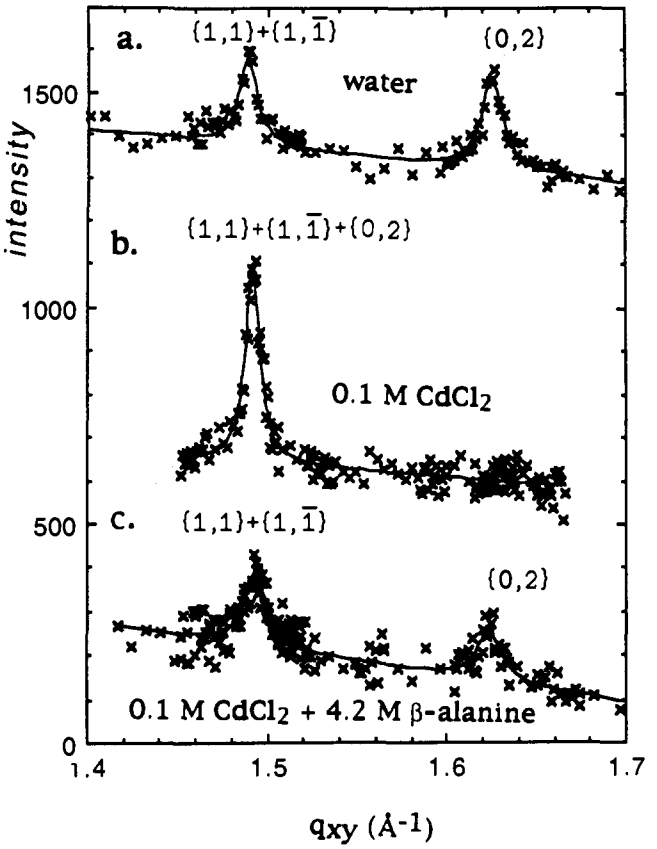


**Figure 8.** GID intensity pattern from a compressed monolayer (30 mN/m) of an equimolar mixture of octadecylamine and stearic acid over various aqueous solutions at a temperature of 5 °C: (a) pure water, (b) 0.1 M $CdCl_2$ solution, and (c) 0.1 M $CdCl_2$ and 4.2 M β-alanine solution. The {*h*,*k*} indices of the reflections are indicated.

translation along the short *a* axis and so molecules of opposite charge are related by "glide" symmetry along the $a + b$ diagonal. In model II the situation is reversed, and the repeat structure is described by a supercell $a_s = 2a$ and $b_s = 2b$. Naturally it is not possible to distinguish between the two models from GID data. The calculated Bragg rod profiles were obtained making use of an X-ray structure factor formula[32-35,37] assuming an atomic coordinate model,[38] with fits shown in Figure 9a.

The GID measurements for the monolayer mixture on the 0.1 M $CdCl_2$ subphase revealed, in terms of the structure on pure water, that the {0,2} reflection disappeared and that the {1,1} + {1,1̄} reflection remained at the same $q_{xy}$ position, and approximately twice as intense (Figure 8a,b). We interpret these results as follows. Making use of monolayer-counterion stoichiometry obtained from the X-ray reflectivity results, in which one $Cd^{2+}$ ion is bound to two carboxylate amphiphiles and one $Cl^-$ to one amine amphiphile, we assume that the structure is composed of alternate rows of long chain carboxylates and amines, as on pure water. We introduce $Cd^{2+}$ and $Cl^-$ ions into the most reasonable sites so that $Cd^{2+}$ ions straddle alternate pair of neighboring $CO_2^-$ groups and $Cl^-$ ions straddle each pair of neighboring $NH_3^+$ groups as shown in Scheme 1. We first considered a model assuming the same supercell $a_s = 2a$ and $b_s$

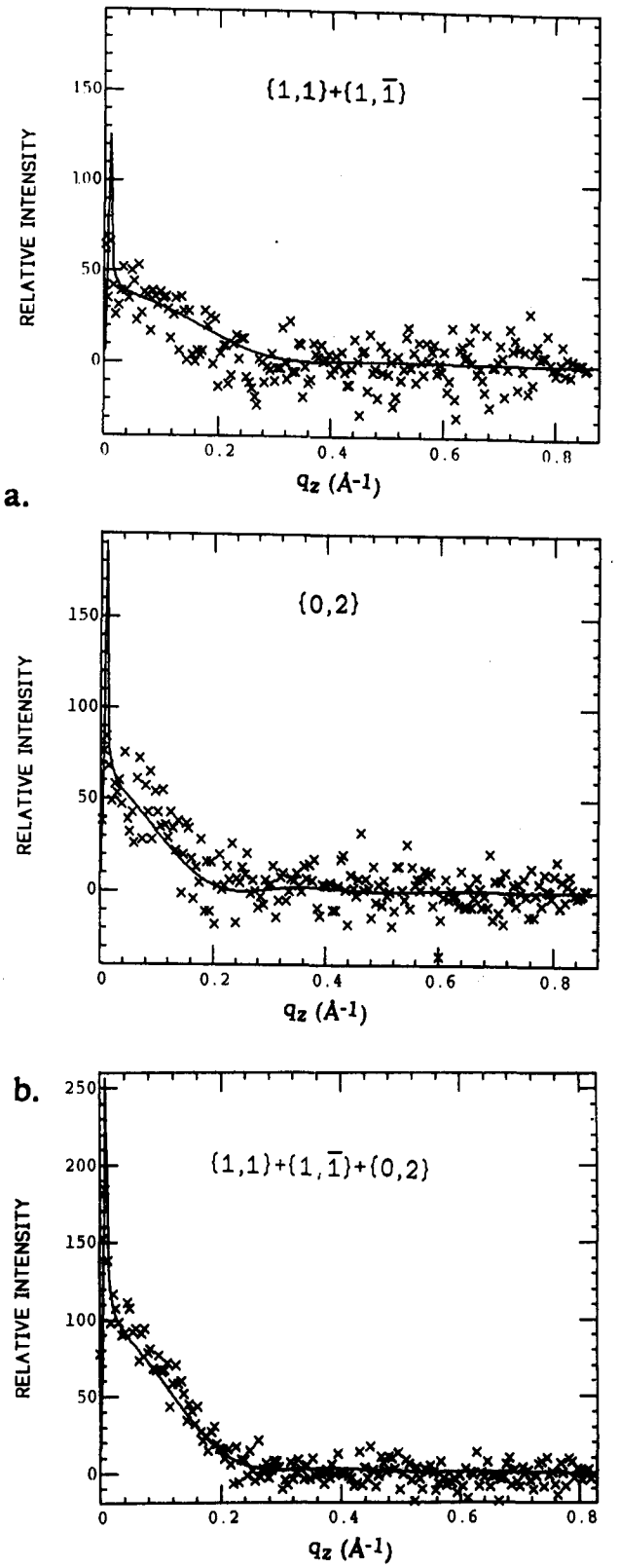


**Figure 9.** Measured (points) and calculated (line) Bragg rod intensity profiles along the vertical scattering vector $q_z$ of the {1,1} + {1,1̄} and {0,2} reflections of the compressed monolayer of the equimolar mixtures of octadecylamine and stearic acid for the two subphases, (a) water and (b) 0.1 M $CdCl_2$ aqueous solution.

$= 2b$ as in model II on pure water, since the one observed reflection remains at the same $q_{xy} = 1.49$ Å$^{-1}$. Note that in terms of this supercell we must reassign the reflection indices so that $\{h_s, k_s\} = \{2h, 2k\}$. In order to account for the absence of the supercell $\{h_s, k_s\}$ reflection {0,4} the neighboring molecular rows parallel to the $a_s + b_s$ diagonal must be offset by $\Delta x_s, \Delta y_s = (0.125, 0.125)$ as shown in Figure 10c. In this arrangement the intensity of the

(37) The variation of the intensity,[38] $I_{hk}(q_z)$, along the Bragg rod as a function of $q_z$ is given by

$$I_{hk}(q_z) = KK'V(q_z)|F_{hk}(q_z)|^2 DW_{hk}(q_z)$$

where $K$ scales the calculated to the observed intensities; $K'$ depends on the crossed beam area, the Lorentz–polarization terms, and the unit cell area; the grazing geometry factor $V(q_z)$ describes the interference of rays diffracted upward with rays diffracted down and subsequently reflected back up by the interface;[39] $F_{hk}(q_z)$ is the molecular structure factor; and $DW_{hk}(q_z)$ is the Debye–Waller factor.

(38) Leveiller, F.; Jacquemain, D.; Leiserowitz, L.; Kjaer, K.; Als-Nielsen, J. *J. Phys. Chem.* **1992**, *96*, 10380.

(39) Vineyard, G. *Phys. Rev.* **1982**, *26*, 4146–4159.

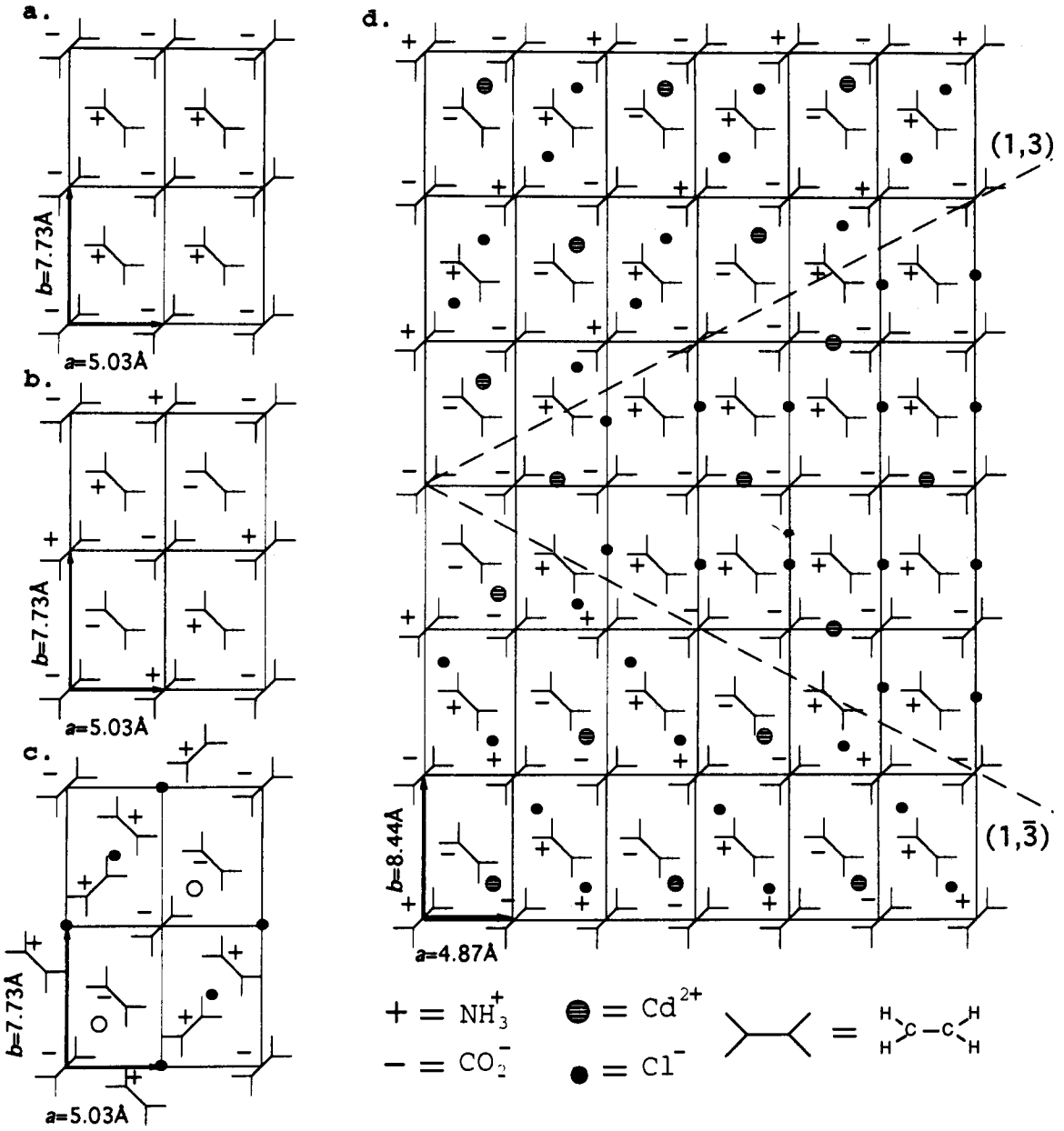


**Figure 10.** Schematic representation of the model packing arrangements of the mixed monolayer of octadecylamine and stearic acid on pure liquid water and bound to $Cd^{2+}$ and $Cl^-$ ions; (a) and (b) Models I and II on pure water. The hydrocarbon chains in the unit cell *a,b* are related by glide symmetry. (c) and (d) Models on $CdCl_2$ solution. In (c) the structure was constructed from model II by offsetting neighboring amphiphilic chains parallel to $a + b$ diagonal. Moreover, the $Cd^{2+}$ ions bridge alternate pairs of neighboring $CO_2^-$ head groups along the $a + b$ direction, the $Cl^-$ ions are intercalated between $NH_3^+$ head groups. Part (d) represents a composite structure constructed assuming twinning of the counterions and the charged head groups about the (1,3) and (1,$\bar{3}$) planes. Note that the hydrocarbon chains are viewed along the chain axis.

**Scheme 1**

Row of $C_{17}H_{35}CO_2^-$ with intercalated $Cd^{2+}$ ions

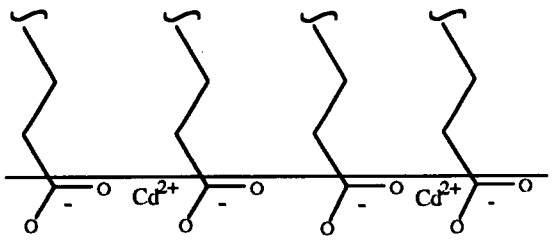


Row of $C_{18}H_{37}NH_3^+$ with intercalated $Cl^-$ ions

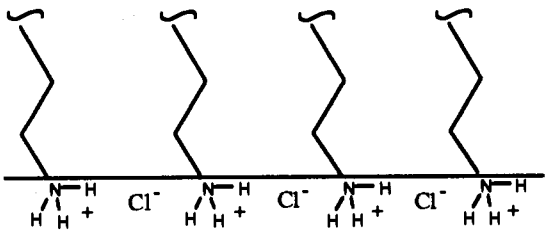


$\{h_s, k_s\}$ reflection $\{0.4\}$ would be very weak, on symmetry grounds, since for each amphiphilic chain at $x_s,y_s,z$ there is another at $x_s + 0.125, y_s + 0.125, z$. Indeed the calculated intensity was very weak, the combined contribution of the $Cd^{2+}$ and $Cl^-$ ions to the Bragg rod being low. But the $\{h_s, k_s\}$ reflection $\{1,1\} + \{1.\bar{1}\}$ cannot be weak on symmetry grounds. Its calculated intensity proved comparable to that of the observed supercell reflection $\{2,2\} + \{2,\bar{2}\}$ at $q_{xy} = 1.49$ Å$^{-1}$. However the supercell reflection $\{1,1\} + \{1,\bar{1}\}$ was not observed in the measured range $q_{xy} = 0.6$–$0.9$ Å$^{-1}$. Thus this model must be discarded.

We now examine the other possibility where the single GID peak obtained over $CdCl_2$ solution arises from a cell in which all

three low-order {h, k} reflections {1,1}, {1,$\bar{1}$}, and {0,2} coincide at the same value of $q_{xy}$ as that of the {1,1} + {1,$\bar{1}$} peak obtained over pure water. This would yield a rectangular cell $a = 4.87$ Å, $b = 8.44$ Å and so an area/molecule $ab/2 = 20.5$ Å$^2$. This value is larger than the unit cell area/molecule of 19.4 Å$^2$ over pure water. At first sight this appears to be unreasonable in view of the strong attractive electrostatic interactions involving the bound $Cd^{2+}$ and $Cl^-$ ions to the amphiphilic $CO_2^-$ and $NH_3^+$ head groups, unless we assume partial intercalation of the counterions between the head groups, leading to some expansion of the cell area. In general, three coinciding base reflections {1,1}, {1,$\bar{1}$}, and {0.2} referring to the rectangular cell $a,b$ indicates a hexagonal cell $a_h = b_h$, $\gamma = 120°$, where $a_h = 0.5(a + b)$, $b_h = 0.5(a - b)$, and implies at least 3-fold symmetry. The question is how may we construct an arrangement with at least "overall" 3-fold symmetry, but which would incorporate the molecular rows depicted in Scheme 1. A possible model embodies a crystal twinned about particular sets of planes, so as to form a continuous mosaic of crystallites. An analogous twinning pattern has been observed in Langmuir monolayers of amphiphilic alcohols $C_nH_{2n+1}OH$ ($n$ = 13–16) on vitreous ice, detected by cryoelectron microscopy.[40] The electron diffraction patterns were observed displaying 6-fold symmetry, with the structures exhibiting rectangular symmetry so that {0,2} reflection had a different $d$-spacing from those of the {1,1} and {1,$\bar{1}$}. These structures were twinned about the {1,3} planes to form the mosaic. We propose a somewhat similar mosaic arrangement of twinned crystallites for the mixed monolayer as shown in Figure 10d. The twinning applies only to the counterions and to carboxylate/amino head groups of the amphiphiles but not to the chains themselves. It is only by virtue of such twinning, which incorporates strongly bound amphiphile-counterion rows (Scheme 1) along the three directions, $a$, $a + b$, and $a - b$, that we may justify a rectangular cell with dimensions compatible with hexagonal symmetry. Perhaps the driving force for the formation of such multiple twinning to yield "overall" trigonal symmetry is that the three different domains are equienergetic. We have no estimate of the domain size within the mosaic. Presumably they should comprise at least 20–30 unit cells in order to behave as an ordered structure. In this respect it is difficult to construct a regular trigonal lattice in which the molecules and counterions are arranged either in ordered positions or in a random manner with reasonable nearest-neighbor contacts of the positively and negatively charged species.

According to the analysis of the reflectivity data, the addition of β-alanine to the $CdCl_2$ solution causes a competitive binding to the monolayer. This result is in keeping with the reappearance of the {0,2} reflection when both $CdCl_2$ and β-alanine are present in solution (Figure 8c) which leaves the unit cell essentially unchanged as it was on water.

## 4. Conclusion

The pronounced change in morphology of β-alanine when grown in the presence of $Cd^{2+}$ and $Cl^-$ ions may be understood in terms of the effect of $CdCl_2$ on the structure of the mixed monolayer of octadecylamine and stearic acid. The head group arrangement of this monolayer mimics to an appreciable extent the crystal face of β-alanine most affected by $CdCl_2$. The X-ray reflectivity and grazing incidence X-ray diffraction measurements indicate that $Cd^{2+}$ and $Cl^-$ ions are bound to the mixed monolayer at ordered sites and induce the formation of a mosaic crystalline pattern with "overall" macroscopic trigonal symmetry. Moreover, β-alanine solute binds in a competitive way to the monolayer and so acts as a scavenger for potential binding sites. Ordered binding of $CdOH^+$ ions to an arachidate monolayer has been reported.[36] This is the first example of a monolayer system in which we have proven the presence of ordered counterions of opposite charges.

**Acknowledgment.** We thank Meir Lahav for support and useful discussions. We also thank Jaroslaw Majewski for pertinent comments. We are grateful to the German-Israeli Foundation, the Danish Foundation for Natural Sciences, and the fund for Basic Research of the Israel Academy of Sciences and Humanities for financial support and Hasylab, DESY, Hamburg, Germany for beam time.

(40) Majewski, J.; Margulis, L.; Jacquemain, D.; Leveiller, F.; Böhm, C.; Arad, T.; Talmon, Y.; Lahav, M.; Leiserowitz, L. *Science* **1993**, *261*, 899–902.